Enzymatic Characterization of the Target for Isoniazid in *Mycobacterium tuberculosis*†

Annaïk Quémard,‡ James C. Sacchettini,§ Andréa Dessen,§ Catherine Vilcheze,|| Robert Bittman,|| William R. Jacobs, Jr.,‡ and John S. Blanchard*,§

Departments of Biochemistry and Microbiology and Immunology, Howard Hughes Medical Institute, Albert Einstein College of Medicine, 1300 Morris Park Avenue, Bronx, New York 10461, and Department of Chemistry and Biochemistry, Queens College, Flushing, New York 11367

Received February 28, 1995; Revised Manuscript Received May 9, 1995®

ABSTRACT: The *inhA* gene has been recently shown to encode a common protein target for isoniazid and ethionamide action in *Mycobacterium tuberculosis*. In this paper, we demonstrate that the *M. tuberculosis* InhA protein catalyzes the NADH-specific reduction of 2-*trans*-enoyl-ACP, essential for fatty acid elongation. This enzyme preferentially reduces long-chain substrates (12−24 carbons), consistent with its involvement in mycolic acid biosynthesis. Steady-state kinetic studies showed that the two substrates bind to InhA via a sequential kinetic mechanism, with the preferred ordered addition of NADH and the enoyl substrate. The chemical mechanism involves stereospecific hydride transfer of the 4*S* hydrogen of NADH to the C_3 position of the 2-*trans*-enoyl substrate, followed by protonation at C_2 of an enzyme-stabilized enolate intermediate. Kinetic and microcalorimetric analysis demonstrates that the binding of NADH to the S94A mutant InhA, known to confer resistance to both isoniazid and ethionamide, is altered. This difference can account for the isoniazid-resistance phenotype, with the formation of a binary InhA−NADH complex required for drug binding. Isoniazid binding to either the wild-type or S94A mutant InhA could not be detected by titration microcalorimetry, suggesting that this compound is a prodrug, which must be converted to its active form.

Isoniazid (INH) was first reported to be effective against *Mycobacterium tuberculosis* and *Mycobacterium bovis* in 1952 (Bernstein et al., 1952; Fox, 1952; Offe et al., 1952; Pansy et al., 1952). Isoniazid alone has been shown to be an effective prophylactic antitubercular (Robitzek & Selikoff, 1952), and the combined administration of isoniazid, rifampicin, and pyrazinamide has proven to be an effective chemotherapeutic regimen for the treatment of drug-sensitive *M. tuberculosis* infections (Combs et al., 1990). Isoniazid-resistant strains were isolated almost immediately after this antibiotic began to be used therapeutically (Middlebrook, 1952), and presently about 20% of the *M. tuberculosis* strains in New York City are resistant to isoniazid (Frieden et al., 1993). Determining the molecular mechanism of action of isoniazid, and its cellular target, thus is crucial both for understanding resistance mechanisms in mycobacteria and for designing more potent antimycobacterial agents for controlling tuberculosis.

Early observations suggested a link between INH resistance and the loss of mycobacterial catalase−peroxidase activity (Cohn et al., 1954; Middlebrook, 1954). Recent reports have demonstrated that deletion of, or point mutations in, the *M. tuberculosis katG* gene, which encodes a unique catalase−peroxidase, results in the acquisition of INH resistance and that transformation of INH-resistant strains of *M. tuberculosis* with a functional *katG* gene restores sensitivity to the drug (Zhang et al., 1992, 1993). A more recent report has shown that the mycobacterial catalase−peroxidase oxidizes isoniazid to form reactive intermediates, which can be quenched with added nucleophiles (Johnsson & Schultz, 1994). Other mechanisms of resistance must exist, however, since isoniazid resistance correlates with a loss of catalase−peroxidase activity in only 20−30% of clinical isolates (Stoeckle et al., 1993; Heym et al., 1994; Kapur et al., 1995).

A novel gene, *inhA*, was identified from *M. tuberculosis*, *Mycobacterium avium*, *Mycobacterium smegmatis*, and *M. bovis* by characterization of genetic variants that conferred resistance to both isoniazid and ethionamide (Banerjee et al., 1994). Resistance to these two antitubercular drugs was shown to be mediated by either mutations in the structural gene or the presence of the wild-type gene on a multicopy plasmid. In two different studies, *ca.* 25% of isoniazid-resistant clinical isolates contained mutations within the *inhA* locus (Heym et al., 1994; Kapur et al., 1995). Consistent with the results of laboratory isolates (Banerjee et al., 1994), mutations in the *inhA* locus were identified both within the structural gene and in the 5′ regulatory region (Heym et al., 1994; Kapur et al., 1995). The amino acid sequence homology of InhA with enzymes involved in bacterial and plant fatty acid biosynthesis made the InhA protein an attractive target for isoniazid action, based on the demonstration that the drug inhibited the biosynthesis of cell wall fatty acids, specifically the mycolic acids, found in mycobacteria and related bacteria (Takayama & Davidson, 1979). Isoniazid has been shown to inhibit the synthesis of mycolic

† Supported by NIH Grants AI33696 (J.S.B.) and AI36849 (W.R.J.) and a fellowship from the Heiser Foundation (A.D.).

* To whom correspondence should be addressed [telephone (718) 430-3096, FAX (718) 892-0703].

‡ Department of Microbiology and Immunology, Albert Einstein College of Medicine.

§ Department of Biochemistry, Albert Einstein College of Medicine.

|| Department of Chemistry and Biochemistry, Queens College.

® Abstract published in *Advance ACS Abstracts,* June 15, 1995.

0006-2960/95/0434-8235$09.00/0 © 1995 American Chemical Society

acids in mycobacterial cells (Takayama et al., 1972) and cell-free extracts (Quemard et al., 1991). In support of this hypothesis, cell-free extracts of mycobacterial strains expressing the S94A mutant InhA showed significantly reduced levels of inhibition of mycolic acid biosynthesis by isoniazid (Banerjee et al., 1994). The sequence homology of InhA with the *Brassica napus* enoyl-ACP reductase (Slabas et al., 1986) led us to suspect that InhA catalyzed a similar reaction. The recent three-dimensional structural determinations of both the wild-type and S94A mutant forms of InhA (Dessen et al., 1995) have encouraged us to perform a detailed enzymatic characterization of the isoniazid target in *M. tuberculosis*.

MATERIALS AND METHODS

Overexpression of InhA Protein in Escherichia coli. The *inhA* gene of *M. tuberculosis* H37Rv was amplified by PCR, using primers which contained *Nco*I and *Bam*HI restriction sites at the 5′ and 3′ ends, respectively. The PCR product was ligated into the pET-15b overexpression vector (Novagen), which had been previously treated with *Nco*I and *Bam*HI restriction enzymes, and this plasmid was used to transform the BL21(DE3) *E. coli* strain (Novagen). No unexpected mutations (the second codon of the *inhA* gene was changed in order to introduce the *Nco*I site into the gene)[1] were introduced into the cloned *inhA* gene as a result of these manipulations, as evidenced by nucleotide sequencing of the inserted gene. For the expression of S94A InhA in *E. coli*, a fragment of the wild-type *M. tuberculosis inhA* gene was replaced in the pET-15b expression plasmid between the *Sfi*I (nt 213) and *Bst*BI (nt 555) restriction sites, by restriction and ligation of its single base-mutated equivalent.

Purification. The *E. coli* BL21(DE3)::*inhA* strain was grown in 4 L of Terrific broth in a high-density fermentor to an OD_{600} of 9 and induced with 1 mM IPTG. At an OD_{600} of 18, 150 g of cells were harvested by centrifugation and frozen at −70 °C. Standard protein purification methods were performed at 4 °C, and fractions were analyzed by SDS−PAGE. Cells were disrupted by sonication, and the supernatant obtained after centrifugation was treated with streptomycin sulfate (1% w/v final) to remove nucleic acids. The supernatant obtained after centrifugation was dialyzed and applied to a 5 × 40 cm Fast-Flow Q Sepharose (Pharmacia) anion-exchange column. Proteins were eluted using a linear 0−1 M NaCl gradient, and fractions containing the InhA protein were pooled, dialyzed, concentrated by ultrafiltration, and applied to a Superdex 75 (Pharmacia) gel filtration column. Fractions containing the InhA protein were pooled and applied to a 1.6 × 10 cm Mono Q (Pharmacia) high-performance anion-exchange column. Elution with a nonlinear 0−0.6 M NaCl gradient yielded fractions which exhibited a single 28.5 kDa band on SDS−PAGE stained with Coomassie Blue (Figure 1B). Concentrated solutions of the homogeneous protein (>10 mg/mL) were colorless, and the extinction coefficient of the protein was determined to be $\epsilon_{280} = 37.3 \pm 0.2\ mM^{-1}\ cm^{-1}$ by amino acid analysis. The purified enzyme is stable in 20 mM PIPES, pH 7.3, containing 50% glycerol at −20 °C for more than 6 months.

[1] The mass of the full-length InhA protein predicted from the gene sequence is 28 547 Da. The purified protein expressed in *E. coli* is posttranslationally proteolyzed with loss of the amino-terminal methionine. For simplicity of cloning into pET vectors at the *Nco*I site, the second amino acid was changed from a Thr to an Ala.

Synthesis and Purification of 2-trans-Enoyl-CoAs and 2-trans-Enoyl-ACP. 2-*trans*-Enoyl-CoAs were synthesized from the corresponding free acid and coenzyme A (CoA) by the mixed anhydride method (Goldman & Vagelos, 1961) and purified by reverse-phase HPLC using a 3.9 × 300 mm C_{18} μBondapak column (Waters) equilibrated in CH_3OH-H_2O containing 0.02 M NaH_2PO_4 and eluted at 1 mL/min with a gradient of CH_3OH (1.33%/min), using detection at 260 nm. The 2-*trans*-alkenoic acids were synthesized from their corresponding alcohols by oxidation with pyridinium chlorochromate (Morisaki et al., 1980). The aldehydes were converted to the alkenoates by a modification of the Wittig reaction using ethyl (triphenylphosphoranylidene)acetate (Monteagudo et al., 1990). Saponification of the esters afforded the 2-*trans*-alkenoic acids, which were purified by reverse-phase HPLC using a 3.9 × 300 mm C_{18} μBondapak column (Waters).

2-*trans*-Octenoyl-ACP was prepared enzymatically using *E. coli* ACP and acyl-ACP synthetase (Rock & Garwin, 1979). The extent of coupling was assessed by determining the residual thiol content of ACP using Ellman's reagent (DTNB). The 2-*trans*-octenoyl-ACP was purified on octyl-Sepharose as described (Rock & Garwin, 1979).

Steady-State Kinetics. Kinetic parameters were determined spectrophotometrically by following NADH oxidation at 340 nm using a thermostated Uvikon 9310 spectrophotometer. All reactions were run in 30 mM PIPES buffer, pH 6.8, at 25 °C. Steady-state K_m values for NADH were determined at variable concentrations of NADH and at fixed concentrations of either 2-*trans*-octenoyl-ACP (10 μM) or 2-*trans*-octenoyl-CoA (215 μM). The maximum velocities and K_m values of 2-*trans*-octenoyl-ACP, 2-*trans*-octenoyl-CoA, 2-*trans*-dodecenoyl-CoA, and 2-*trans*-hexadecenoyl-CoA were determined at variable concentrations of the reducible substrate and at a fixed, saturating concentration of NADH (100 μM). Crotonoyl-CoA was tested at concentrations up to 8 mM. Data were plotted in Lineweaver−Burk reciprocal form and fitted to eq 1, using the Fortran programs of Cleland

$$v = VA/(K + A) \quad (1)$$

(1979). Initial velocity studies were performed by varying the concentration of NADH at several fixed concentrations of 2-*trans*-dodecenoyl-CoA. Data were plotted in reciprocal form and fitted to eq 2. Product inhibition studies were

$$v = VAB/(K_{ia}K_b + K_aB + K_bA + AB) \quad (2)$$

performed by varying the concentration of product inhibitor versus one of the substrates at a fixed concentration of the other substrate. Data were plotted in reciprocal form and fitted to eq 3, which describes linear competitive inhibition.

$$v = VA/(K(1 + I/K_{is}) + A) \quad (3)$$

Primary Deuterium Kinetic Isotope Effect. [(4*S*)-4-^{2}H]-NADH and [(4*R*)-4-^{2}H]NADH were prepared enzymatically and purified as previously described (Sweet & Blanchard, 1991). Initial velocities for the oxidation of reduced nucleotide were measured spectrophotometrically in the presence of either 10 μM 2-*trans*-octenoyl-ACP or 100 μM 2-*trans*-octenoyl-CoA. Data were plotted in reciprocal form and fitted to eq 4, which assumes nonequivalent primary deuterium kinetic isotope effects on V, E_V, and V/K_{NADH}, $E_{V/K}$.

$$v = VA/(K(1 + E_{V/K}) + A(1 + E_V) \quad (4)$$

Initial velocity patterns were also obtained using NADH or [(4*S*)-4-^{2}H]NADH as the variable substrate in the presence of several fixed concentrations of 2-*trans*-dodecenoyl-CoA. The data were fitted individually to eq 2, and the fitted parameters V, K_{ia}, V/K_a and V/K_b, obtained using either NADH or [(4*S*)-4-^{2}H]NADH, were compared.

Titration Microcalorimetry. InhA (98 μM) in 20 mM Hepes, pH 7.3, was titrated with 3.03 mM NADH in the same buffer in an Omega microcalorimeter (MicroCal, Inc.), by 25 successive injections of 4 μL, at 25 °C. S94A InhA (95 μM) in 20 mM Hepes, pH 7.3, was titrated with 3.03 mM NADH in the same buffer by 50 successive injections of 4 μL, at 23 °C. The stoichiometry of nucleotide binding and the K_d value were determined using the MicroCal ORIGIN 2.9 software supplied with the instrument.

Mass Spectrometry. Electrospray ionization mass spectrometry was performed on octyl-Sepharose-purified samples of ACP and fatty acyl-ACP derivatives in an API III triple quadrapole mass spectrometer (PE Sciex) after desalting of the samples on a Waters C8 reverse-phase column. The data were deconvoluted to determine the molecular weights of the various species.

Three-Dimensional Structure and Modeling. The three-dimensional structure of the NADH binary complexes of InhA and the S94A mutant was recently determined (Dessen et al., 1995). The E−NADH−substrate analog complex was modeled using manual fitting with the Insight program, and the figures were prepared using the program SETOR (Evans, 1993).

RESULTS AND DISCUSSION

The *M. tuberculosis* InhA protein was expressed in *E. coli* by cloning the corresponding gene in a pET vector. Growth of the resulting strain and induction with 1 mM IPTG resulted in the expression of InhA as a soluble protein of 28.5 kDa (monomeric size), comprising *ca.* 20% of the total soluble protein as determined by SDS−PAGE (Figure 1A).

Approximately 200 mg of homogeneous InhA was obtained from a 4 L culture of the *E. coli* strain by standard purification methods (Figure 1B). Amino-terminal sequencing confirmed the identity of the purified protein as the *inhA* gene product. The absence of detectable protein impurities and the molecular weight of the protein were determined by SDS−PAGE and LC/electrospray MS. The protein exhibits a molecular mass of 28 368 Da, in agreement with the mass predicted from the gene sequence.[1] The enzyme exists as a homodimer in solution. The S94A mutant enzyme was expressed and purified in a manner identical to that described for the wild-type enzyme and elutes from gel filtration columns at the same position as the wild-type enzyme.

Catalytic activity was demonstrated spectrophotometrically when preparations of 2-*trans*-octenoyl-ACP were tested as a substrate, identifying the *inhA* gene product as a fatty enoyl-ACP reductase. This activity was linearly dependent on the concentration of InhA added. The octyl-Sepharose-purified 2-*trans*-octenoyl-ACP and the precursor ACP were analyzed by electrospray ionization mass spectrometry. ACP exhibited a mass of 8849 (Figure 2A), while the 2-*trans*-octenoyl-ACP exhibited a mass of 8973 (Figure 2B), as expected for the addition of the octenoate moiety (mass 125) to the covalently

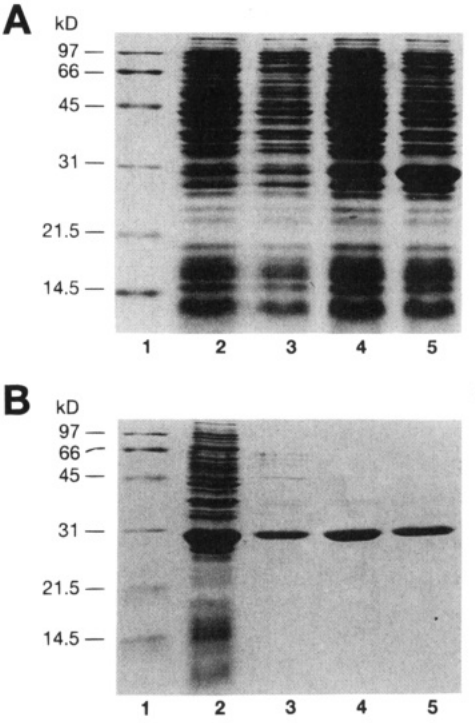

FIGURE 1: Overexpression and purification of InhA protein. (A) SDS−PAGE analysis of crude extracts of *E. coli* strains: (1) molecular mass markers; (2) BL31(DE3); (3) BL21(DE3) treated for 1 h with 1 mM IPTG; (4) BL21(DE3)::*inhA*; (5) BL21(DE3)::*inhA* treated for 1 h with 1 mM IPTG. (B) SDS−PAGE analysis of InhA purification: (1) molecular mass markers; (2) cell-free extract of BL21(DE3)::*inhA* treated with IPTG; (3) pooled fractions after Fast-Flow Q Sepharose anion-exchange chromatography; (4) pooled fractions after Superdex 75 gel filtration chromatography; (5) pooled fractions after Mono Q high-performance anion-exchange chromatography.

bound phosphopantetheine group of ACP. The InhA-catalyzed reduction of 2-*trans*-octenoyl-ACP by NADH yielded the saturated product, octanoyl-ACP, with a predicted, and observed, molecular mass 2 mass units greater than 2-*trans*-octenoyl-ACP (Figure 2C).

The steady-state kinetic parameters for the InhA-catalyzed reduction of 2-*trans*-octenoyl-ACP are shown in Table 1. These values are similar to steady-state Michaelis constants for NADH and crotonoyl-ACP reported for the *B. napus* and *E. coli* enoyl-ACP reductases (Slabas et al., 1986; Bergler et al., 1994). 2-*trans*-Octenoyl-CoA was shown to be an alternate substrate for InhA, exhibiting a steady-state K_m value approximately 2 orders of magnitude higher than the K_m value for 2-*trans*-octenoyl-ACP (Table 1) but a similar maximum velocity. In order to determine the chain-length specificity of InhA, we measured the steady-state kinetic parameters exhibited by 2-*trans*-dodecenoyl-CoA and 2-*trans*-hexadecenoyl-CoA (Table 1). The C_{16} derivative is a far better substrate than octenoyl-CoA, displaying a K_m value 2 orders of magnitude lower than the C_8, and with dodecenoyl-CoA exhibiting intermediate behavior. Substrate specificity studies of InhA with longer chain enoyl-CoAs were difficult due to their low critical micellar concentrations. Comparisons of the initial rates of NADH oxidation at a single, low (1 μM) concentration of enoyl-CoA of various chain lengths showed that the C_{20} and C_{24} enoyl-CoAs were at least as good substrates as dodecenoyl-CoA (Figure 3). No reaction could be demonstrated with crotonoyl-CoA, even at a crotonoyl-CoA concentration as high as 8 mM. Although

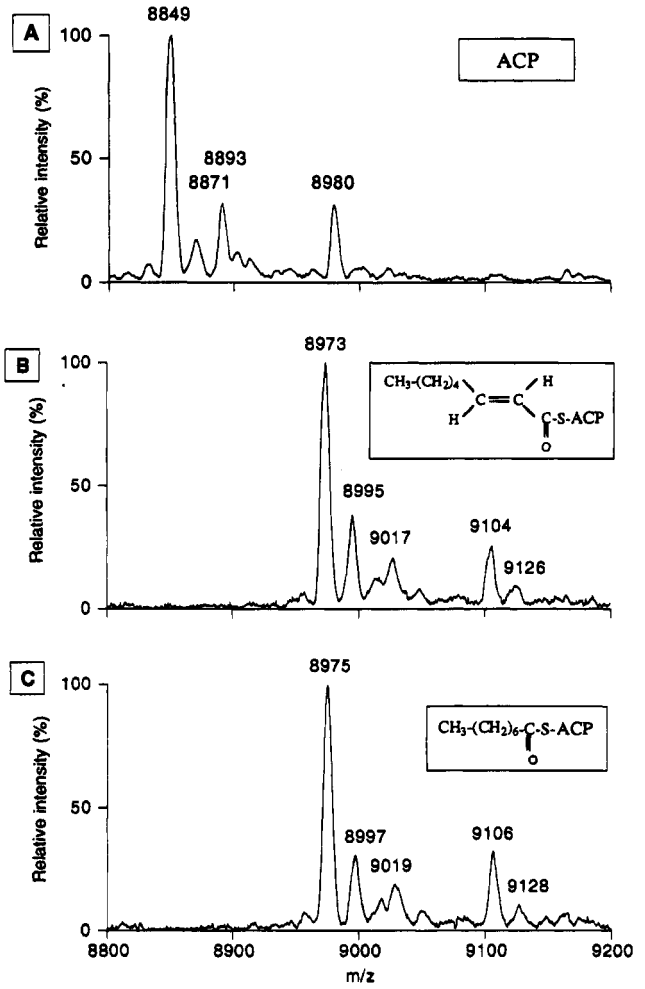

FIGURE 2: Electrospray ionization–mass spectrometry of precursor, substrate, and product of the InhA-catalyzed reaction. (A) Mass spectrum of *E. coli* acyl carrier protein (ACP, Sigma). (B) Mass spectrum of 2-*trans*-octenoyl-ACP. (C) Mass spectrum of the product of the NADH-dependent reduction of 2-*trans*-octenoyl-ACP by InhA protein. In all spectra, the [M − 1 + 23], [M − 2 + 46], [M − 1 + 132], and [M − 1 + 132 + 23] ions represent the molecular ion [M] with a single bound sodium ion, two bound sodium ions, and the amino-terminally methionylated ACP with or without a single bound sodium ion.

Table 1: Kinetic Parameters of *M. tuberculosis* InhA

substrate	wild-type InhA	S94A InhA
2-*trans*-octenoyl-ACP		
K_m (μM)	2.0 ± 0.4	2.7 ± 1.0
NADH K_m (μM)	8.1 ± 0.1	37.3 ± 1.7
V_{max} (μmol min^{-1} mg^{-1})	2.2 ± 0.4	3.1 ± 0.6
2-*trans*-octenoyl-CoA		
K_m (μM)	467 ± 90	688 ± 197
NADH K_m (μM)	7.6 ± 0.5	65 ± 10
V_{max} (μmol min^{-1} mg^{-1})	3.6 ± 0.5	4.0 ± 0.7
2-*trans*-dodecenoyl-CoA		
K_m (μM)	48 ± 6	
V_{max} (μmol min^{-1} mg^{-1})	5.8 ± 0.5	
2-*trans*-hexadecenoyl-CoA		
K_m (μM)	1.5 ± 0.2	
V_{max} (μmol min^{-1} mg^{-1})	4.5 ± 0.3	

InhA has significant sequence homology to the enoyl-ACP reductases from *B. napus* and *E. coli* (EnvM), it differs from both enzymes by its specificity for long-chain fatty acyl substrates, since both the *B. napus* and *E. coli* enoyl-ACP reductases accept crotonoyl-CoA as a substrate at concentrations as low as 100 μM (Slabas et al., 1986; Bergler et al., 1994).

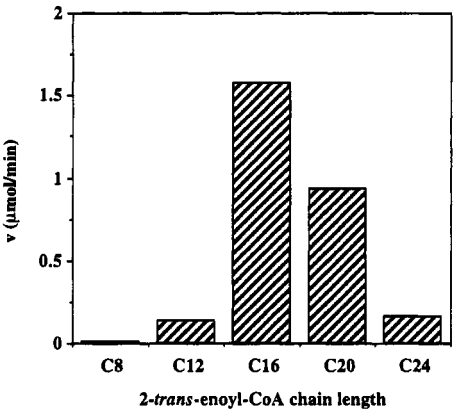

FIGURE 3: Chain-length specificity for enoyl-CoA substrates. The initial rate of reduction by wild-type InhA was measured in the presence of 1 μM 2-*trans*-enoyl-CoA and a saturating concentration of NADH. The number of carbons in the different enoyl chains is specified on the graph.

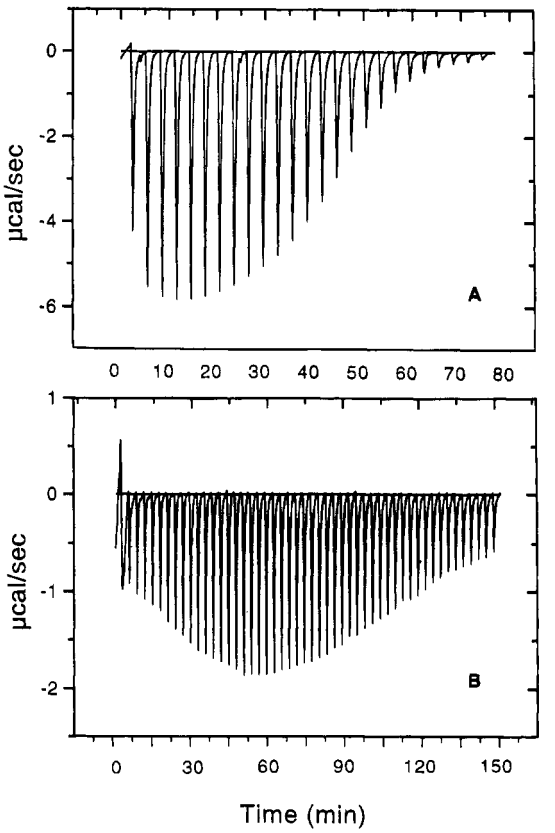

FIGURE 4: Microcalorimetric titration of NADH binding to wild-type and S94A InhA. (A) Wild-type InhA. The K_d value, determined from a fit of four independent experiments to a single-site model, was 2 ± 0.8 μM, with a determined stoichiometry of 1.0 ± 0.1 per 28.5 kDa.[2] (B) S94A InhA. The K_d values, determined from a fit of the experimental results to a two-site model, were 27 and 89 μM, respectively, to the first and second site.

Initial velocity studies, determined by varying the concentration of NADH at several fixed levels of dodecenoyl-CoA, displayed a pattern of intersecting lines when plotted in reciprocal fashion, indicating the sequential addition of the two substrates to InhA. NAD^+ is a linear competitive inhibitor versus NADH (K_{is} = 4 ± 1 mM), suggesting that both NADH and NAD^+ bind to the free enzyme. To confirm and extend these kinetic observations, we examined NADH

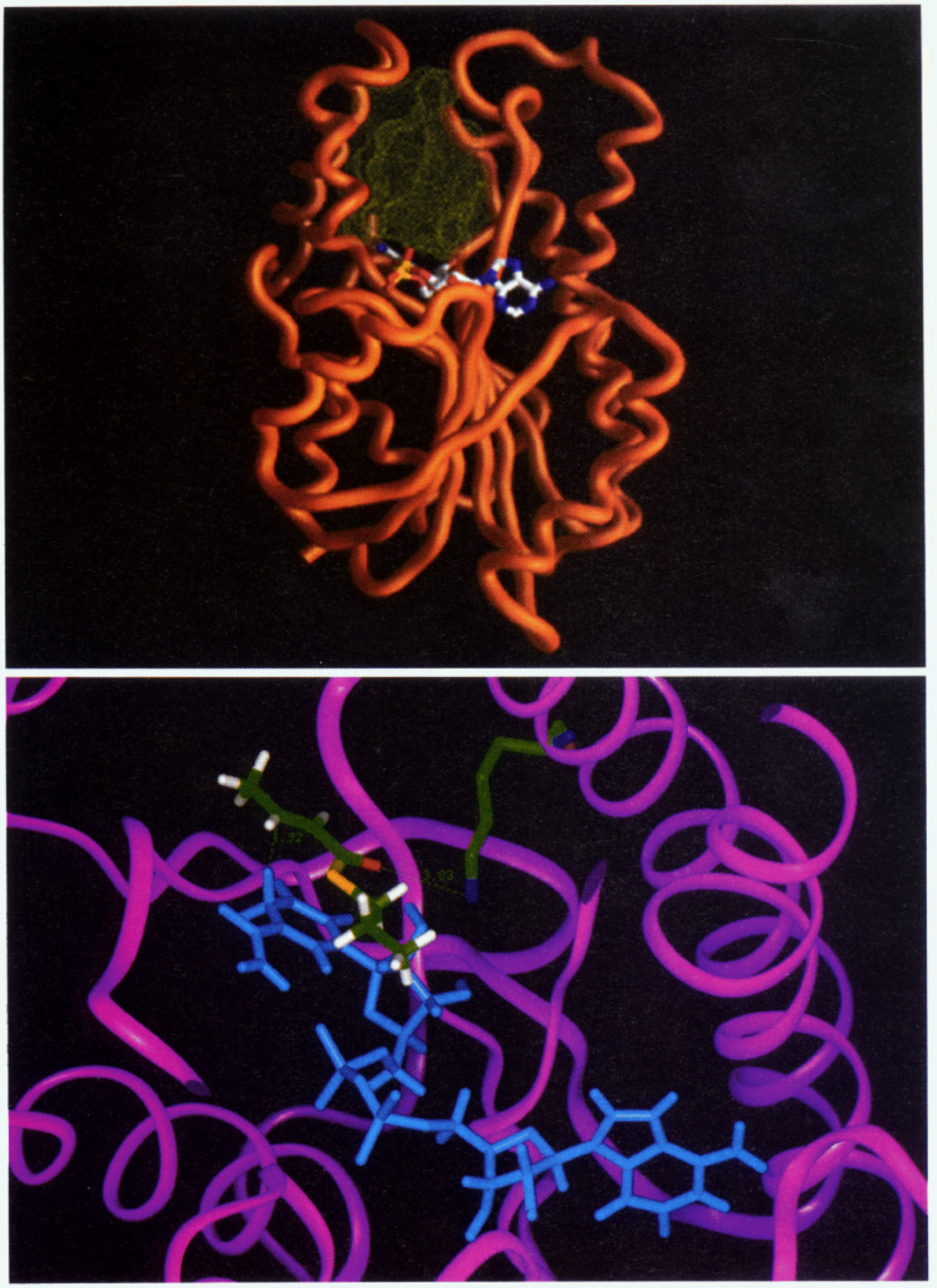

FIGURE 5: Structures of the InhA−NADH complex and the active site. (A, top) Trace of the main chain of InhA (Dessen et al., 1995, orange ribbon) showing the bound NADH, colored by atom type (nitrogen, blue; oxygen, red; phosphorus, yellow; carbon, white), and the interior hydrophobic cavity (shown as a yellow stippled surface). (B, bottom) Modeling of the binding of an enoylthioester (crotonoyl-*S*-propanethiol) in the active site. The InhA backbone is represented as a purple ribbon. Lys165 and the enoylthioester are shown colored by atom type: nitrogen, blue; oxygen, red; sulfur, yellow; carbon, green; hydrogen, white. NADH is shown in light blue. The distance between the 4*S* hydrogen of NADH and C3 of the modeled substrate is 1.92 Å, while the distance between the carbonyl of the thioester and the ω-amino group of Lys165 is 3.83 Å.

binding to the wild-type enoyl reductase using titration microcalorimetry. NADH exhibits tight, and stoichiometric, binding to wild-type InhA in the absence of the enoyl substrate (Figure 4A).[2]

The stereochemistry of hydride transfer was determined by comparing the rates of reduction of 2-*trans*-octenoyl-ACP by [(4*S*)-4-^{2}H]NADH and [(4*R*)-4-^{2}H]NADH. A kinetic isotope effect of 2.9 ± 0.2 was observed on both V and V/K_{NADH} when rates of [(4*S*)-4-^{2}H]NADH oxidation were compared to the rate of [(4*R*)-4-^{2}H]NADH oxidation at a fixed, nonsaturating concentration of 2-*trans*-octenoyl-ACP of 10 μM, suggesting that hydride transfer is catalyzed from the 4*S* hydrogen to the C_3 position of 2-*trans*-octenoyl-ACP

[2] Neither NADPH, $NADP^+$, nor NAD^+ exhibited demonstrable binding to the wild-type enzyme under these microcalorimetric conditions (K_d > 250 μM). Only weak inhibition by NAD^+ (K_{is} = 4 mM), ADP-ribose, ADP, or AMP could be demonstrated kinetically (data not shown).

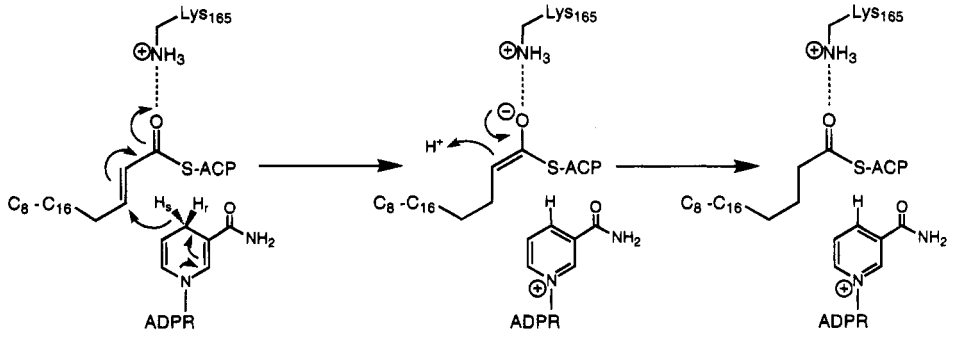

FIGURE 6: Proposed chemical mechanism of *M. tuberculosis* 2-*trans*-enoyl-ACP reductase.

and may be a slow step in the overall reaction. Similar results have been reported for the stereochemistry of hydride transfer catalyzed by enoyl-ACP reductases from bacteria and yeast (Saito et al., 1981). Having determined the stereochemistry of hydride transfer, we sought to distinguish between ordered and random kinetic mechanisms by determining the primary deuterium kinetic isotope effects on the kinetic parameters for 2-*trans*-dodecenoyl-CoA reduction using NADH or [(4*S*)-4-^{2}H]NADH. At fixed, saturating concentrations of NADH or [(4*S*)-4-^{2}H]NADH (150 μM), equivalent isotope effects on V and $V/K_{2\text{-}trans\text{-}\text{dodecenoyl-CoA}}$ of 3.8 ± 0.1 were obtained using 2-*trans*-dodecenoyl-CoA as the variable substrate. This experiment was repeated using variable concentrations of NADH or [(4*S*)-4-^{2}H]NADH at several fixed levels of 2-*trans*-dodecenoyl-CoA, and the two data sets (^{1}H or ^{2}H) were fit to eq 2 to obtain values for the kinetic parameters. Poorly defined values of ^DV and $^DK_{ia}$ were obtained, but $^DV/K_{NADH}$ and $^DV/K_{2\text{-}trans\text{-}\text{dodecenoyl-CoA}}$ were well-defined and equal to 2.3 ± 0.4 and 4.6 ± 0.5, respectively. The nonunitary value of $^DV/K_{NADH}$ suggests that the kinetic mechanism is not strictly ordered with this long-chain enoyl substrate (Cook & Cleland, 1981) but that there is a preferred order of addition, with NADH binding preceding enoyl substrate binding.

These results are supported by the three-dimensional structure of the binary InhA−NADH complex (Dessen et al., 1995) that reveals that the 4*S* hydrogen of bound NADH is oriented away from the protein surface and toward a large cavity (Figure 5A). The abundance of hydrophobic and aromatic side chains and the volume of this cavity (*ca.* 580 Å^3) make it the likely binding site for medium- to long-chain fatty acyl substrates. Docking of a simple substrate analog, crotonoyl-*S*-propanethiol, showed that a bound fatty enoylthioester, oriented in order to position its C_3 within 2 Å of the 4*S* hydrogen of NADH, and the fatty acyl chain oriented in the cavity, could form a reasonable hydrogen bond between the substrate carbonyl oxygen and Lys165 (Figure 5B). This hydrogen bond could facilitate hydride transfer by polarizing the carbonyl group and conjugated carbon−carbon double bond, promoting catalysis and stabilizing enolate formation. Similar hydrogen bonding between a tyrosyl hydroxyl group and the carbonyl group of substrates of ketosteroid isomerase has been proposed to explain the polarization of the substrate during catalysis (Austin et al., 1992). Similarly, Raman spectroscopic investigations suggest a high degree of polarization of the thioester carbonyl of α,β-unsaturated substrate analogs bound to the mechanistically related enoyl-CoA hydratase (D'Ordine et al., 1994). These data permit us to propose a chemical mechanism for the InhA-catalyzed, NADH-dependent reduction of 2-*trans*-enoyl-ACP by the direct transfer of the 4S hydrogen atom of NADH to the C_3 position of the α,β-unsaturated thioester, with the intermediate formation of an enzyme-stabilized enolate anion. Collapse of the enolate via protonation at C_2 would yield the observed, saturated product (Figure 6).

Kinetic evaluation of the S94A InhA-catalyzed reduction of 2-*trans*-octenoyl-ACP, or 2-*trans*-octenoyl-CoA, by NADH revealed that the steady-state K_m values of the enoyl substrates and the maximum velocity were not significantly different from these parameters determined with the wild-type protein. A specific effect of the mutation is the 5−10-fold higher steady-state Michaelis constant for NADH (Table 1). These data suggest that the S94A mutation affects the steady-state binding of NADH, perhaps via a reduction in the affinity of the enzyme for the reduced nucleotide. Kinetic results reported for nucleotide binding to the related enoyl-ACP reductase encoded by *E. coli envM* (Bergler et al., 1994) have shown that nucleotide binding was required for binding of the antibiotic, diazaborine. A mutant enzyme, obtained by selection for diazaborine resistance in *E. coli*, exhibited substantially reduced nucleotide affinity. To confirm and extend our kinetic observations, we performed titration microcalorimetry on the S94A mutant InhA (Figure 4B). The binding of NADH to the S94A mutant InhA appears to be cooperative, and a fit of the data to a two-site model yielded K_d values for the binding of NADH to the two nucleotide binding sites in the dimer that are significantly higher than the K_d value obtained with the wild-type InhA. These results are in agreement with the higher, kinetically determined, K_m values observed for the S94A mutant InhA (Table 1). These preliminary thermodynamic studies are being extended to obtain more detailed information concerning the mechanism of cooperative binding of NADH to the S94A mutant enzyme. However, structural comparisons of the wild-type and S94A mutant InhA have revealed that this mutation occurs in the nucleotide binding region and that the side-chain hydroxyl of Ser94 interacts with an ordered water molecule, which in turn is hydrogen bonded to one of the oxygen atoms of the pyrophosphoryl moiety of NADH (Dessen et al., 1995). In the mutant, this interaction is lost, and changes in the orientation of Gly14, located in loop 1, cause small, but potentially significant, structural changes.

The direct binding of isoniazid, *kat*G-generated isoniazid metabolites (e.g., isonicotinic acid or 4-pyridinecarboxaldehyde; Johnsson & Schultz, 1994), or ethionamide to either enoyl-ACP reductase or the reductase−NADH complex could not be detected by titration microcalorimetry. In steady-state kinetic experiments, we have shown isoniazid to be a poor inhibitor of the enzymatic activity (K_{is} *ca.* 40

mM vs 2-*trans*-octenoyl-CoA). This suggests that isoniazid, *per se*, is not the active form of the drug but rather a prodrug, which must be converted to an active form in order to interact with InhA. Isoniazid is known to be metabolically unstable in mycobacteria (Ratledge, 1982; Youatt & Tham, 1969), and it has been shown that the *M. tuberculosis* catalase–peroxidase oxidizes isoniazid to an electrophilic species which can react with various nucleophiles (Johnsson & Schultz, 1994). If activated isoniazid binding to, and inactivation of, InhA is dependent on the presence of bound NADH, then the reduced affinity for NADH by the S94A mutant can fully account for the resistance phenotype observed in cells expressing the S94A mutant (Banerjee et al., 1994). Thus, given the low *in vivo* concentrations of free NADH in *M. tuberculosis* H37Rv (estimated at <10 μM; Gopinathan et al., 1963), a 5–10-fold increase in the steady-state Michaelis constant for NADH can easily account for the 10-fold increase in the MIC for isoniazid in isoniazid-resistant cells. These isoniazid-resistant strains must be able to accommodate the lower rate of enoyl reduction as a result of the S94A mutation, and either this step is not rate limiting in the biosynthesis of long-chain fatty acids or the organism can raise the intracellular NADH concentration to maintain the biosynthetic flux, since the maximum velocity exhibited by the mutant is unchanged from the wild type.

The combination of previously reported genetic (Banerjee et al., 1994) and structural (Dessen et al., 1995) evidence and the present enzymological data lead us to propose that InhA is the primary target of isoniazid action in *M. tuberculosis*. The long-chain enoyl-ACP reductase activity of InhA is entirely consistent with its involvement in mycolic acid biosynthesis. It is possible that InhA is part of the type II ACP-dependent fatty acid synthetase system described previously (Matsumura et al., 1970) in *M. smegmatis*. This system differs from the conventional procaryotic fatty acid synthesis systems by its specificity for long-chain (C_{12}–C_{18}) primers which are elongated to form C_{18}–C_{30} acyl-ACP products which may serve as precursors to the even longer C_{40}–C_{60} fatty acyl chains present in *M. tuberculosis* mycolic acids. The data contained here suggest that InhA is the first enzyme target for a clinically relevant antibacterial compound involved in fatty acid biosynthesis. We suggest that a KatG-generated isoniazid metabolite could interact with, and inhibit, the enoyl-ACP reductase encoded by the *inhA* gene. Alternative mechanisms for the *in vivo* activation of isoniazid, which are independent of KatG-dependent oxidation, may additionally generate enoyl-ACP reductase inhibitors, since isoniazid-sensitive strains of *M. tuberculosis* with no catalase–peroxidase activity have been isolated (Stoeckle et al., 1993). A more complete understanding of these activation processes, in combination with the available three-dimensional structures of both wild-type and S94A InhA (Dessen et al., 1995), should hasten the development of compounds which will be effective against both isoniazid-sensitive and -resistant strains of *M. tuberculosis*.

ACKNOWLEDGMENT

We are grateful to David and Eugenie Dubnau for helpful discussions, Asesh Banerjee for providing the *M. tuberculosis inhA* gene, and E. Nieves and X. Tang for assistance in obtaining the electrospray ionization mass spectra.

REFERENCES

Austin, J. C., Kuliopoulos, A., Mildvan, A. S., & Spiro, T. G. (1992) *Protein Sci. 1*, 259.

Banerjee, A., Dubnau, E., Quemard, A., Balsubramanian, V., Um, K. S., Wilson, T., Collins, D., de Lisle, G., & Jacobs, W. R. (1994) *Science 263*, 227.

Bergler, H., Wallner, P., Ebeling, A., Leitinger, B., Fuchsbichler, S., Aschauer, H., Kollenz, G., Hogenauer, G., & Turnowsky, F. (1994) *J. Biol. Chem. 269*, 5493.

Bernstein, J., Lott, W. A., Steinberg, B. A., & Yale, H. L. (1952) *Am. Rev. Tuberc. 65*, 357.

Cleland, W. W. (1979) *Methods Enzymol. 63*, 103.

Cohn, M. L., Kovitz, C., Oda, U., & Middlebrook, G. (1954) *Am. Rev. Tuberc. 70*, 641.

Combs, D. L., O'Brien, R. J., & Geiter, L. J. (1990) *Ann. Intern. Med. 112*, 397.

Cook, P. F., & Cleland, W. W. (1981) *Biochemistry 20*, 1790.

Dessen, A., Quemard, A., Blanchard, J. S., Jacobs, W. R., Jr., & Sacchettini, J. C. (1995) *Science 267*, 1638.

D'Ordine, R. L., Tonge, P. J., Carey, P. R., & Anderson, V. E. (1994) *Biochemistry 33*, 12635.

Evans, S. V. (1993) *J. Mol. Graphics 11*, 134.

Fox, H. H. (1952) *Science 116*, 129.

Frieden, T. R., Sterling, T., Pablos-Mendez, A., Kilburn, J. O., Cauthen, G. M., & Dooley, S. W. (1993) *N. Engl. J. Med. 328*, 521.

Goldman, P., & Vagelos, P. R. (1961) *J. Biol. Chem. 236*, 2620.

Gopinathan, K. P., Sirsi, M., & Ramakrishnan, T. (1963) *Biochem. J. 87*, 444.

Heym, B., Honore, N., Truffot-Pernot, C., Banerjee, A., Schurra, C., Jacobs, W. R., Jr., van Embden, J. D. A., Grosset, J. H., & Cole, S. T. (1994) *Lancet 344*, 293.

Johnsson, K., & Schultz, P. G. (1994) *J. Am. Chem. Soc. 116*, 7425.

Kapur, V., Ling-Ling, L., Hamrick, M R., Plikaytis, B. B., Shinnick, T. M., Telenti, A., Jacobs, W. R., Jr., Banerjee, A., Cole, S., Yuen, K. Y., Clarridge, J. E., Kreiswirth, B. N., & Musser, J. M. (1995) *Arch. Pathol. Lab. Med. 119*, 131.

Matsumura, S., Brindley, D. N., & Bloch, K. (1970) *Biochem. Biophys. Res. Commun. 38*, 369.

Middlebrook, G. (1952) *Am. Rev. Tuberc. 65*, 765.

Middlebrook, G. (1954) *Am. Rev. Tuberc. 69*, 471.

Monteagudo, E. S., Burton, G., & Gros, E. G. (1990) *Helv. Chim. Acta 73*, 2097.

Morisaki, M., Shibata, M., Duque, C., Imamura, N., & Ikekawa, N. (1980) *Chem. Pharm. Bull. 28*, 606.

Offe, H. A., Siefkin, W., & Domagk, G. (1952) *Z. Naturforsch. 76*, 462.

Pansy, F., Stander, H., & Donovick, R. (1952) *Am. Rev. Tuberc. 65*, 761.

Quemard, A., Lacave, C., & Laneelle, G. (1991) *Antimicrob. Agents Chemother. 35*, 1035.

Ratledge, C. (1982) in *The Biology of the Mycobacteria* (Ratledge, C., & Stanford, J., Eds.) Vol. 1, pp 185–271, Academic Press, London.

Robitzek, E. H., & Selikoff, I. J. (1952) *Am. Rev. Tuberc. 65*, 402.

Rock, C. O., & Garwin, J. L. (1979) *J. Biol. Chem. 254*, 7123.

Saito, K., Kawaguchi, A., Seyama, Y., Yamakawa, T., & Okuda, S. (1981) *Eur. J. Biochem. 116*, 581.

Slabas, A. R., Sidebottom, C. M., Hellyer, A., Kessell, R. M. J., & Tombs, M. P. (1986) *Biochim. Biophys. Acta 877*, 271.

Stoeckle, M. Y., et al. (1993) *J. Infect. Dis. 168*, 1063.

Sweet, W. L., & Blanchard, J. S. (1991) *Biochemistry 30*, 8702.

Takayama, K., & Davidson, L. A. (1979) in *Antibiotics* (Hahn, F. E., Ed.) Vol. V, pp 98–119, Springer-Verlag, New York.

Takayama, K., Wang, L., & David, H. L. (1972) *Antimicrob. Agents Chemother. 2*, 29.

Youatt, J., & Tham, S. H. (1969) *Am. Rev. Respir. Dis. 100*, 77.

Zhang, Y., Heym, H., Allen, B., Young, D., & Cole, S. (1992) *Nature 358*, 591.

Zhang, Y., Garbe, T., & Young, D. (1993) *Mol. Microbiol. 8*, 521.

BI950464N